The second data release of the Indian Pulsar Timing Array: Investigating the Effect of Coronal Mass Ejection on PSR J1022+1001 and a Possible Mode Change of PSR J2145-0750

Shaswata Chowdhury,^a M. A. Krishnakumar,^b Manjari Bagchi,^{a,c} Bhal Chandra Joshi,^{d,e} Nobleson K.,^f Jibin Jose,^g Shantanu Desai,^h Manpreet Singh,ⁱ Vaishnavi Vyasraj,^h Kuldeep Meena,^j Amarnath,^k Manoneeta Chakraborty,^g Shubham Kala,^a Debabrata Deb,^l Zenia Zuraiq,^m Arul Pandian B,^{k,n} Neelam Dhanda Batra,^o Churchil Dwivedi,^p Sushovan Mondal,^{a,c} Avinash Kumar Paladi,^m Kaustubh Rai,^q Abhimanyu Susobhanan,^r Adya Shukla,^e Aman Srivastava,^{s,h} Mayuresh Surnis,^q Hemanga Tahbildar,^q Keitaro Takahashi,^f Pratik Tarafdar,^t Prabu Thiagaraj,^k and Kunjal Vara^q

 ^aThe Institute of Mathematical Sciences, C. I. T. Campus, Taramani, Chennai 600113, India
 ^bRadio Astronomy Centre, National Centre for Radio Astrophysics, Tata Institute of Fundamental Research, Udhagamandalam, Tamil Nadu, 643001, India

 $[^]c\mathrm{Homi}$ Bhabha National Institute, Training School Complex, Anushakti Nagar, Mumbai 400094, India

 $[^]d {\rm National}$ Centre for Radio Astrophysics, SP Pune University Campus, Pune, Maharashtra, 411007, India

^eDepartment of Physics, Indian Institute of Technology Roorkee, Roorkee, Uttarakhand, 247667, India

 $[^]f{\rm Faculty}$ of Advanced Science and Technology, Kumamoto University, 2-39-1 Kurokami, Kumamoto 860-8555, Japan

 $[^]g$ Department of Astronomy, Astrophysics, and Space Engineering, Indian Institute of Technology Indore, Indore 453552, India

^hDepartment of Physics, IIT Hyderabad, Kandi, Telangana 502284, India

ⁱDepartment of Physical Sciences, Indian Institute of Science Education and Research (IISER) Mohali, Sector 81, SAS Nagar, Mohali, Punjab, 140306, India

jUM-DAE Centre for Excellence in Basic Sciences, University of Mumbai, Vidyanagari, Mumbai 400098, India.

E-mail: shaswata.phyres@gmail.com

Abstract. The Indian Pulsar Timing Array (InPTA) has recently published its second data release (DR2), comprising the timing analysis of seven years of data on 27 millisecond pulsars (MSPs), observed simultaneously in the 300-500 MHz (band 3) and 1260-1460 MHz (band 5), using the upgraded Giant Metrewave Radio Telescope (uGMRT). The low-frequency data, particularly in band 3, is highly sensitive to propagation effects such as dispersion measure (DM) fluctuations, which can be imprints of some astrophysical phenomena (scientific outliers). Here, we analyze the two outliers of possible astrophysical origin coming from the band 3 DM time series of two pulsars: PSR J1022+1001, with an ecliptic latitude of -0.06°, and PSR J2145-0750, one of the brightest MSPs, with multi-component profile morphology. Our study reveals compelling evidence for a coronal mass ejection (CME) event traced in the data of PSR J1022+1001, and reports evidence for a potential mode-changing event in PSR J2145-0750. Extending the analyses presented here to the full sample of InPTA-DR2 pulsars is expected to reveal additional CME events, and possible mode-changing events. Such detections will not only improve our understanding of solar and pulsar magnetospheric plasma interactions but will also enable more accurate modelling of DM variations, leading to improved pulsar timing solutions, which are crucial for high-precision Pulsar Timing Array (PTA) science.

^kRaman Research Institute, Bengaluru 560080, Karnataka, India

^lCentre for Space Research, North-West University, Private Bag X6001, Potchefstroom 2520, South Africa

^mDepartment of Physics, Indian Institute of Science, C. V. Raman Avenue, Bengaluru 560012, India

ⁿDepartment of Physics and Electronics, The Christ (Deemed to be University), Bangalore, India

^oDepartment of Physics, Indian Institute of Technology Delhi, Hauz Khas, New Delhi 110016

 $[^]p{\rm Astronomy}$ and Astrophysics Division, Physical Research Laboratory, Thaltej Campus, Ahmedabad 380059, Gujarat, India

^qDepartment of Physics, IISER Bhopal, Bhauri Bypass Road, Bhopal, 462066, India

^rMax Planck Institute for Gravitational Physics (Albert Einstein Institute), Callinstraße 38, D-30167 Hannover, Germany

^sDepartment of Physics, GLA University, Mathura 281406, India

 $[^]t \rm INAF$ - Osservatorio Astronomico di Cagliari, via della Scienza 5, 09047 Selargius (CA), Italy

\mathbf{C}	onte	ents	
1	Introduction		
2	Obs	servations and Analysis	2
3	Investigating the effect of CMEs on PSR J1022+1001		
	3.1	Identifying the possible CME affected observations	3
	3.2	CME responsible for the DM outlier	4
	3.3	In situ data	5
	3.4	DM excess estimate	7
4	Analyzing a possible mode change epoch of PSR J2145-0750		8
	4.1	Peak-ratio distribution	9
	4.2	Profile evolution with frequency	9
	4.3	Eliminating systematics degenerate with mode change	10
	4.4	Indication of potential intrinsic magnetospheric changes	11
5	5 Conclusions		14

1 Introduction

High-precision timing of radio pulsars in applications such as the search for low-frequency gravitational waves (GWs) using pulsar timing array experiments (PTAs) often faces the challenge of dealing with shifts in time-of-arrival (ToA) of the radio pulse [1]. Such shifts can be caused by variations in the propagation delay through the ionized inter-stellar medium (IISM) – extreme scattering events [2], scintillations [3, 4], as well as through interplanetary medium (IPM) – coronal mass ejection (CME) [5], solar wind (SW) [6–8], being a few of the explored phenomenons. Such shifts can also be caused by an intrinsic change in the pulse profile from the usually stable standard profile due to glitches [9, 10], magnetospheric origins [11], or mode change [12], but not the stochastic variations. This reveals a systematic shift in the timing residual obtained after a comparison of the observed ToA with that predicted by a model of the pulsar incorporating astrometric, spin, propagation, and binary parameters. Therefore, these "outliers" may indicate astrophysical events of interest, which may be one-off transient events or longer time scale events. A couple of good examples are the profile change event in PSR J1713+0747 reported in 2018 [13], 2020 [14], and 2021 [15] (subsequent interpretations can be found in [11, 16]) and the CME-event reported in PSR J2145-0750 [17].

These profile changes can affect the estimated dispersion measure (DM: a measure of the propagation delay, proportional to the integrated column density of electrons in the inter-stellar and inter-planetary medium along the line-of-sight to the pulsar) of the pulsars. Finding and understanding the causes of such outliers in the DM time series is very important. First, it might lead to serendipitous discovery of interesting astronomical events like profile shape change of the pulsar. Second, it has the potential to improve our understanding of how different astrophysical phenomena impact each other, e.g., coronal mass ejection changing

¹which we refer to as template profile.

the DM of a pulsar. Such outlier events could also affect noise modelling and degrade the sensitivity to gravitational wave searches [18]. Such studies from one pulsar timing experiment (the Indo-Japanese pulsar timing array (InPTA) [19, 20] in the present case) can potentially alert other PTAs to investigate their data, following the example of the profile change event on PSR J1713+0747. As PTA data can be used not only for the detection of low-frequency GWs, but also be used for various other purposes, like improving solar system ephemeris [21–24], testing theories of gravity [25–28], improving the mass measurements of the neutron stars [29] and much more, understanding of outliers in the PTA data is always necessary.

Such outliers can easily be determined through the decade-long monitoring of millisecond pulsars (MSPs) in the PTA experiments. Currently, six such experiments are ongoing with time baselines ranging from 4 years to 28 years (European Pulsar Timing Array (EPTA) [30], the InPTA [19, 20], the Parkes Pulsar Timing Array (PPTA) [31], North American Nanohertz Observatory for Gravitational Waves (NANOGrav) [32], Meerkat Pulsar Timing Array [33] and the Chinese Pulsar Timing Array (CPTA) [34]). The data and resources from these PTA experiments are pooled together by the International Pulsar Timing Array (IPTA) [35] to form the most sensitive data set for the search for GWs. These experiments have reported evidence for the low frequency GWs [33, 36–39].

Recently, InPTA made its second data release (DR2) public [40] with seven years of data on 27 MSPs. This work investigates outliers in the DM time-series of two pulsars from the InPTA DR2 sample and evaluates their potential astrophysical origin. The two pulsars of interest, highlighted here, are – (a) PSR J1022+1001, which has a very low ecliptic latitude of -0.06°, and is known for exhibiting significant solar wind-induced DM variability due to its close proximity to the Sun, making it a natural candidate for probing solar events such as coronal mass ejections; (b) PSR J2145-0750, one of the brightest pulsars in the InPTA sample, shows pronounced short-timescale variations in its DM time series, and its multicomponent profile morphology allows sensitive tests for intrinsic mode-changing behaviour.

The outline of this paper is as follows. We provide an overview of the observational strategy of InPTA DR2 and the analysis carried out in this paper, in Section 2. In Section 3 the investigation for the detection of CME using PSR J1022+1001 data is demonstrated, while in Section 4 we describe the analysis for a potential mode change in PSR J2145-0750. The implications of the results and future directions are discussed in Section 5.

2 Observations and Analysis

The InPTA has been monitoring 27 MSPs routinely using simultaneous observations in the 300–500 MHz (band 3) and 1260–1460 MHz (band 5) with a bandwidth of 200 MHz [40, 41]. The unique subarray capability of the upgraded Giant Metrewave Radio Telescope (uGMRT) [42] is utilized by InPTA to achieve this concurrency. The GMRT antennae are split into two phased arrays with 10 and 15 antennae in band 3 and 5 respectively. The data were recorded with the coherent dedispersion [43] mode at band 3 and using incoherent dedispersion at band 5. Therefore, high precision epoch-wise DM time series is obtained by the InPTA with these data. It may be noted that InPTA is the only PTA experiment which is capable of obtaining instantaneous DM measurements using 300 to 1500 MHz concurrent wide-band observations, unlike other PTA experiments, which utilize multiple epochs to carry out low and high frequency observations. Data on these 27 MSPs over a time baseline of seven years were processed and analyzed. This was published recently as part of InPTA Data

release 2 [40]. In this paper, we use the intermediate and final products of this data release for further investigations. The observing setup, observing strategy and data processing used in InPTA are described in [40, 41, 44], where the reader can find additional details.

The starting point of our analysis, in this paper, is the DM time series from InPTA DR2 - the DM for any given pulsar, for any given epoch was evaluated using DMCalc [17]. Instead of treating every DM outlier as a potential candidate, we define outliers of interest using astrophysical criteria tailored to each case study, as will be explained in the following sections. The candidate outlier for PSR J1022+1001 is cross-checked against solar probe data, coronagraph images, and solar wind simulations. Consistency between enhanced electron densities, CME trajectories, and the pulsar's line of sight is used to validate the association. For PSR J2145-0750, we investigate whether any outlier is instead linked to intrinsic profile evolution. The epoch singled out by the peak-ratio distribution is studied in frequency-resolved folded profiles (300–500 MHz), allowing us to establish if the observed profile departs from the standard template in a manner consistent with mode change. This targeted approach enables us to highlight one astrophysically significant outlier for each of the two pulsars, avoiding the ambiguity of treating all statistical outliers equally. We also briefly examined whether any of the DM outliers could be influenced by terrestrial effects such as lightning or terrestrial gamma-ray flashes (TGFs), which are known to cause short-lived ionospheric perturbations [45] and radio emissions around 300–400 MHz [46], overlapping with our observing band. No consistent correlations were found, suggesting that these effects do not significantly impact our observing bands of interest. In the following sections, we explain the methodology and results in detail for the two pulsars of interest.

3 Investigating the effect of CMEs on PSR J1022+1001

A CME is a large-scale eruption of magnetized plasma from the Sun's corona that expels bulk of charged particles into interplanetary space. To assess whether the identified DM outlier in PSR J1022+1001 is associated with such a solar energetic event, we examine its context in a step-wise manner. We first determine the outlying epochs most likely to be affected by CMEs, then identify candidate CME events from solar monitoring databases. Next, we check for corroborating signatures in in situ solar wind measurements, before finally estimating the expected DM excess contributed by such an event. This structured approach allows us to systematically test the solar origin of the observed anomaly.

3.1 Identifying the possible CME affected observations

We first determined the angular separation between the Sun and the pulsar's line of sight at all observing epochs. To track solar wind related variability, we subtracted the median DM from the epoch-wise DM values – we will refer to this difference as 'observational' DM from here onwards. We then examined the variations in observational DMs as a function of solar elongation. In parallel, we estimated the DM contribution expected from a spherically symmetric solar-wind model using the NE_SW , parameter obtained from the timing solution [40]. This DM is subtracted from its median across the DR2 baseline – we refer to this difference as 'modelled' DM. We refer to the difference between the 'modelled' and 'observational' DM as the DM-excess.

The modelled DM curve was plotted alongside the observational DM values, enabling the identification of 'outlier' epochs. We flagged outliers as those within 20° of the Sun where the observational DM exceeded the model expectation by more than 3σ . This procedure when

carried out on PSR J1022+1001, showed promising signature of a solar event, see Fig. 1. The corresponding MJD is 59800 (09 August 2022), with a separation angle of 17.75° and a DM-excess of 2.91×10^{-3} pc/cc. The profile for this epoch has no visible deviation from its template profile, thereby ruling out any intrinsic origin for such DM-excess.

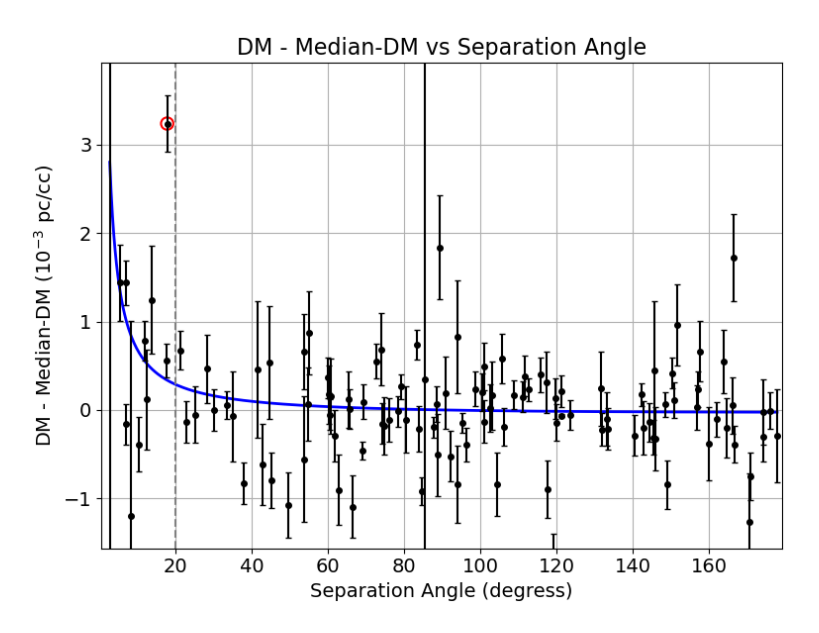


Figure 1: 'Observational' DM and 'modelled' DM vs separation angle (with respect to Sun) for PSR J1022+1001, with the outlier of interest being marked with red circle. The black points represent 'observational' DM, while the blue curve denotes the 'modelled' DM from the spherically symmetric solar wind model.

3.2 CME responsible for the DM outlier

To identify the most plausible CME event(s) that could give rise to such DM-excess, we consulted the DONKI² [47] database for solar eruptive events for three days prior to MJD 59800. From this list, we assess which modelled CMEs are likely to intersect the pulsar's line of sight (LOS), and whether they are simultaneously accessible to any spacecraft capable of providing in situ plasma measurements. Two CME events – cme1, and cme2, emerge as relevant candidates. Both were detected by the Solar TErrestrial RElations Observatory (STEREO)-A spacecraft [48], which at the time was located at 0.95 AU from the Sun with a Heliocentric Earth Ecliptic (HEE) latitude of 0.12° and longitude of –21.97°. The main properties of these events are summarized in Table 1.

To further evaluate the influence of these CMEs on the pulsar's LOS, we turn to visualizations of the DONKI simulations performed within the WSA-ENLIL+Cone (WEC) framework [49–51]. Fig. 2 shows the LOS of PSR J1022+1001 overlaid on the simulation snapshot at 06:00:00 (UTC) on 09 August 2022 (the CME-affected epoch). Given the 6-hour temporal resolution of the simulation, which is much longer than the 17-minute observation duration of the pulsar on that day, this snapshot corresponds to the closest available time

²The Space Weather Database Of Notifications, Knowledge, Information (DONKI), developed at the Community Coordinated Modeling Center (CCMC), is a comprehensive on-line tool for space weather forecasters, scientists, and the general space science community – https://kauai.ccmc.gsfc.nasa.gov/DONKI/.

CME	cme1	cme2
lat	-23.0°	-33.0°
long	-44.0°	-35.0°
speed (km/s)	912	776
half-width	39.0°	20.0°
start-time (UT)	06-08-2022T01:48	07-08-2022T11:00

Table 1: Properties of CMEs that could have affected PSR J1022+1001 observation. The latitude (lat) and longitude (long), in Stonyhurst heliographic coordinate system, represent the direction along which the nose of the individual CMEs propagate. These CME parameters are taken from the DONKI database.

to the actual observation time (05:18:39 UTC) on 09 August 2022. The figure displays the positions of the Sun, Earth, satellites, LOS of the PSR J1022+1001, all projected onto the ecliptic plane – the Sun is marked with a white circle at the centre, while the Earth is marked with a yellow circle, 1 AU away from the centre, along the 0° longitude; the projection of the LOS of PSR J1022+1001 is shown with the yellow line, while those for the satellites and planets are shown with varying colours. The first CME (cme1), associated with a dense, fast outflow, passes beyond both the LOS and STEREO-A, as shown in Fig. 2. The second CME (cme2), however, marginally intersects the LOS during the InPTA observation window, and may represent either a compressed solar wind structure trailing cme1 or a weaker independent event. In either case, it is cme2 that is temporally coincident with the anomalous DM behaviour, because of its influence on the pulsar's LOS on the observation time. The position of the satellites are obtained from the STEREO Science Center, maintained by the National Aeronautics and Space Administration (NASA)³.

Additional support comes from the Large Angle and Spectrometric Coronagraph – C3 (LASCO/C3 coronagraph) [52] data. The base-difference images generated from the corresponding FITS files are carefully oriented with solar north upwards and the Sun centered in the frame. These reveal large-scale outflows associated with the CME events. For PSR J1022+1001, the CME event of interest, i.e., cme2 manifests as a clear mass outflow aligned toward the pulsar LOS. See Fig. 3. In this figure, the pulsar is marked as a red dot, with a dotted line indicating the direction in which the CME should travel to influence the pulsar's LOS. The LASCO/C3 field of view extends to $\sim 8^{\circ}$ from the Sun's center; PSR J1022+1001 lies at an angular separation of 17°, and hence falls outside the image plane. Nevertheless, the inferred trajectory of the CME is consistent with an impact on the LOS.

3.3 In situ data

The in situ data from STEREO-A reveals that the cme1, after starting from the Sun at 06-08-2022 01:48, with a speed of 900 km/s reaches STEREO-A around 08-08-2022 00:00 UTC; we see an enhancement around that time in the measured speed and temperature of the solar wind (see Fig. 4 - generated using CDAWeb⁴). The full data coverage is however missing due to some unknown reason, which could be the reason we do not see the expected jump in the plasma density. Nevertheless, we see subsequent increases in the plasma density after

³https://stereo-ssc.nascom.nasa.gov/cgi-bin/make_where_gif

⁴Coordinated Data Analysis Web (CDAWeb) is part of NASA's Space Physics Data Facility (SPDF), which serves as a central archive and access point for heliophysics and space weather data from various NASA and international missions - https://cdaweb.gsfc.nasa.gov/

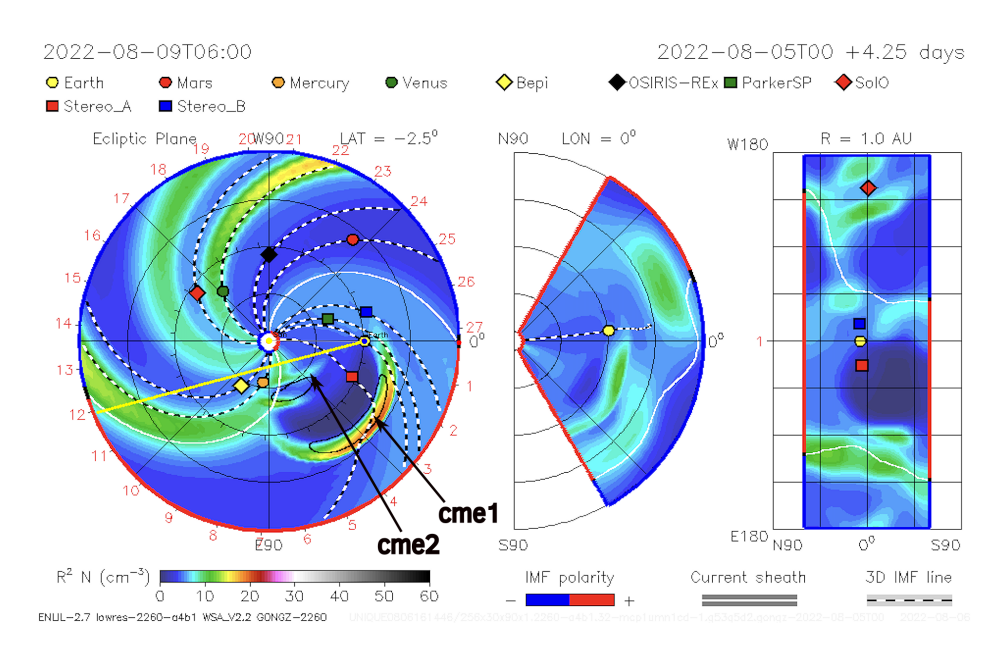


Figure 2: PSR J1022+1001's LOS (yellow line) overlaid on the MHD simulation snapshot taken at 06:00:00 (UTC), around the pulsar observation time on 09 August 2022. Locations of various planets and satellites are shown with different symbols as explained in the legends. The dashed spirals are the Parker spirals, the colour code represent the density as per the colorbar. The two CMEs – cme1, and cme2 are also labelled. These snapshots are taken from the MHD simulations in DONKI.

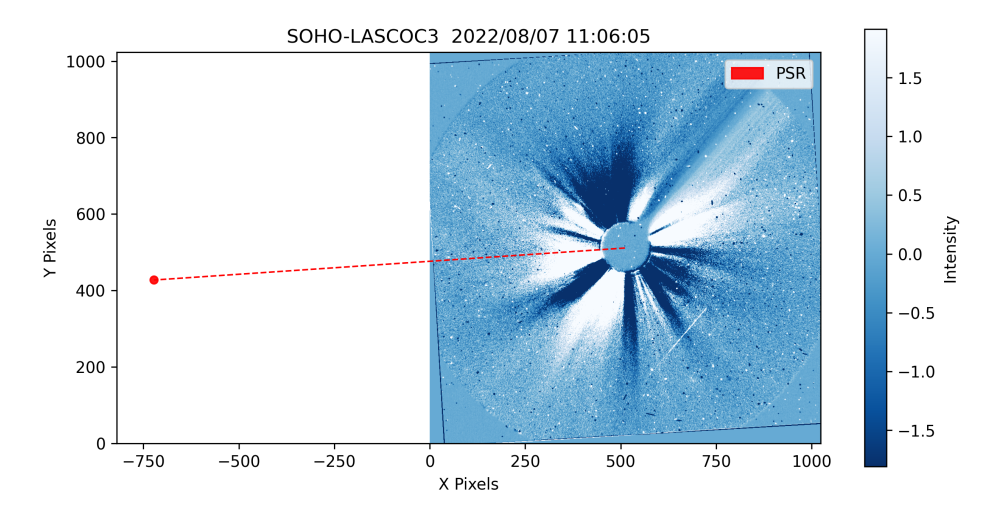


Figure 3: LASCO/C3 coronagraph base difference image plotted from the fits file corresponding to the date of cme2, which passed through the LOS of PSR J1022+1001.

10-08-2022 00:00 UTC, which notably corresponds to the cme2, which after starting from the Sun at 07-08-2022 11:00 UTC, with a speed of 776 km/s is supposed to reach STEREO-A around 09-08-2022 17:00 UTC. The differences in the actual arrival time of the CME and the calculated one lie in the simplistic assumptions, such as constant velocity, which is not completely valid given the fact that CME can accelerate or decelerate along its path due to the drag force [53–55]. The second CME (cme2) seems to be a possible secondary CME coming from nearly the same active region (as cme1, see Table 1), that got accelerated by possible interaction with the fast solar wind component.

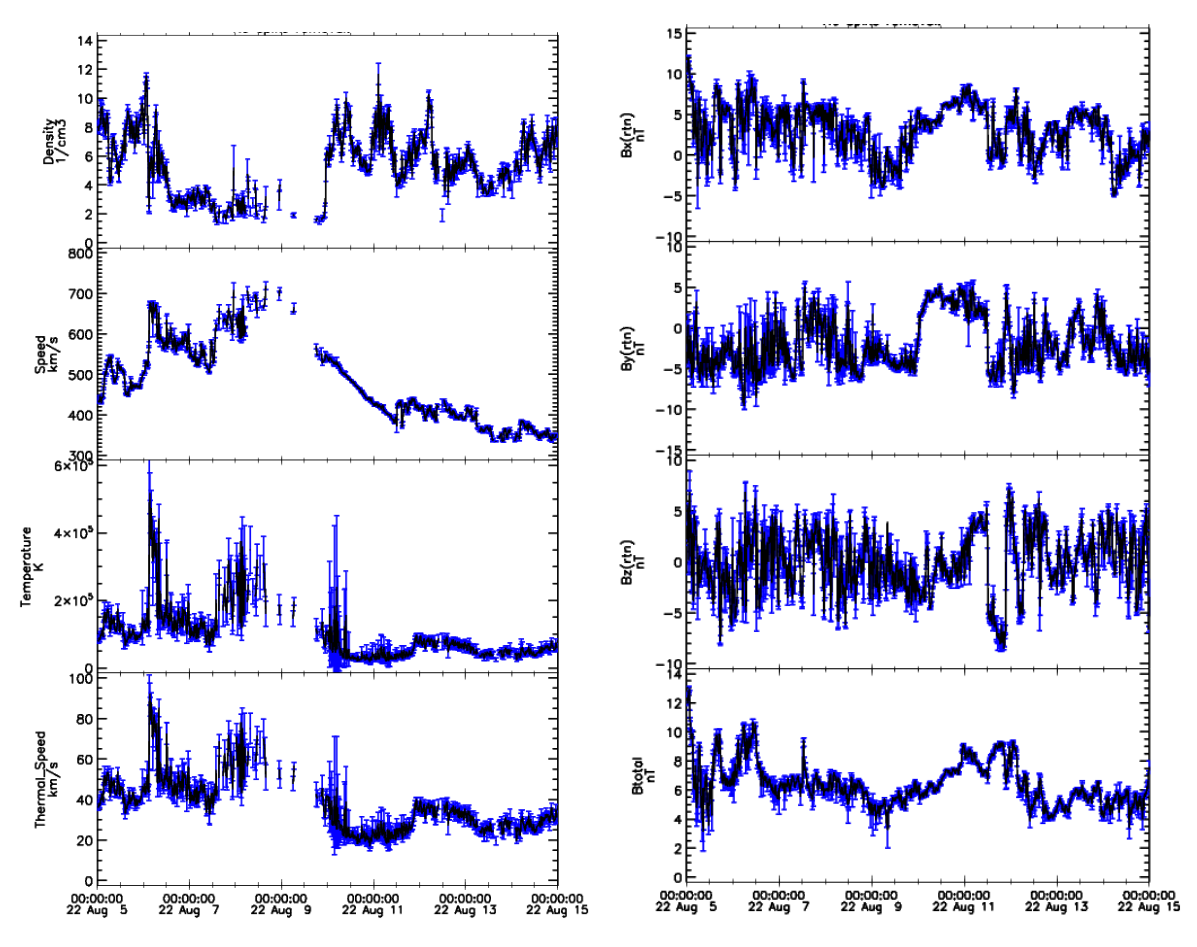


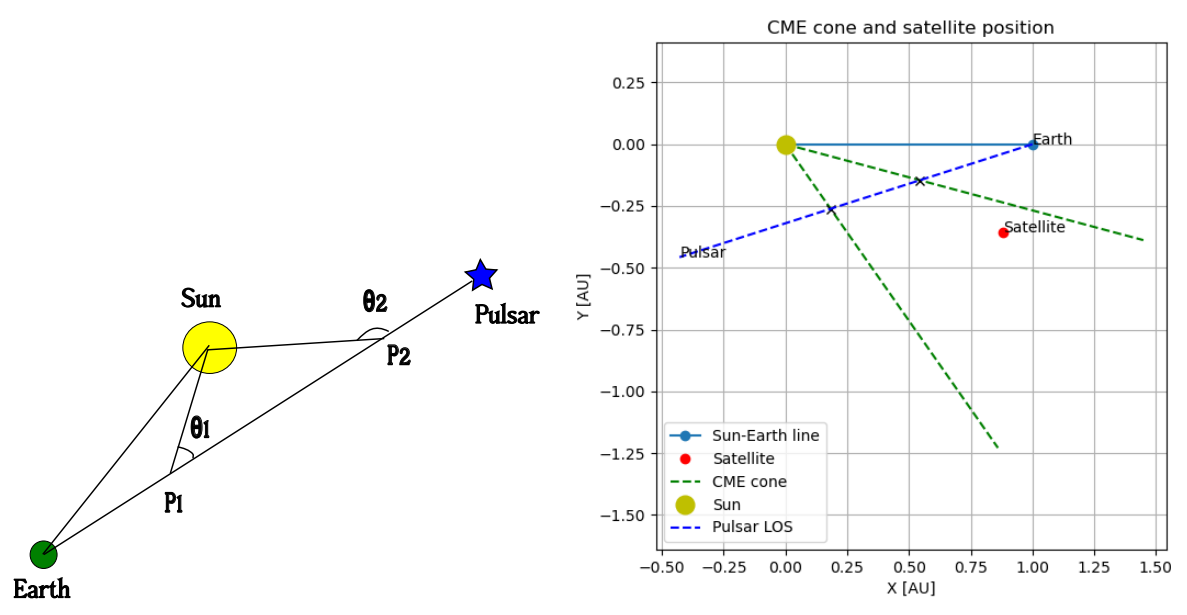
Figure 4: In situ data from STEREO-A for a span of 10 days around the cme2 event is shown. The left panel shows the plasma density in cm⁻³, SW speed, Temperature, and the thermal speed. The right panel shows the measured magnetic field in X,Y and Z directions as well as the total value, in units of nT. These plots are generated using the CDAWeb.

3.4 DM excess estimate

Here, we estimate the DM-excess from the in situ data and the spherically symmetric SW model. From a spherically symmetric SW model consideration, the formula for the DM contribution coming from a portion of the LOS, say P_1 - P_2 (see Fig. 5a) is

$$DM_{P_1 - P_2} = \frac{n_{sat}(r_{sat}(AU))^2}{1 \text{ AU}} \int_{\theta_1}^{\theta_2} d\theta, \qquad (3.1)$$

where n_{sat} is the electron density at the position of the satellite of interest, r_{sat} (AU) is the distance of the satellite from the Sun in units of AU, θ_i is the angle subtended by the sun- P_i line on the earth-pulsar LOS, where $i \in \{1, 2\}$.



- (a) Schematic illustration of integrating-path for DM evaluation
- (b) Propagation path of CME affecting the LOS for PSR J1022+1001

Figure 5: Geometry of paths: (a) DM estimation and (b) impact of CME on LOS of PSR J1022+1001

Using the position coordinates of the satellite of interest, the pulsar's LOS, and the properties of the CME modelling as per DONKI, we identify the portion of the LOS that gets influenced by the cme2's impact on the day of our CME-affected-observation, see Fig. 5b.

The n_{sat} from the in situ data of STEREO-A is roughly 10 cm⁻³. Integrating along the affected portion of the LOS, in Eq. 3.1, we get the DM due to both the CME and the background SW $\sim 5.7 \times 10^{-3}$ pc cm⁻³. From the in situ data over a long time baseline, the background electron density on average is ~ 5 cm⁻³. From this, the DM excess expected due to the background SW is 2.8×10^{-3} pc cm⁻³. Hence the DM-excess from the in situ data is $\sim 2.9 \times 10^{-3}$ pc/cc. This value conforms with the excess DM observed for PSR J1022+1001 on 09 August 2022 (see Section 3.1).

4 Analyzing a possible mode change epoch of PSR J2145-0750

PSR J2145-0750 is one of the brightest pulsars in the InPTA sample, with a distinct multicomponent profile morphology, making it a natural candidate to investigate profile stability in detail. The DM time series of PSR J2145-0750 shows a lot of small-time-scale deviations around its median value, with a prominent outlier lying well below the median belt (see Fig. 6). Interestingly, not all of these deviations are due to poor detection – there is a significant number of such data points showing good detection with high S/N, indicating the possibility of profile showing marginal variability w.r.t. its template. To examine further, we proceeded as follows.

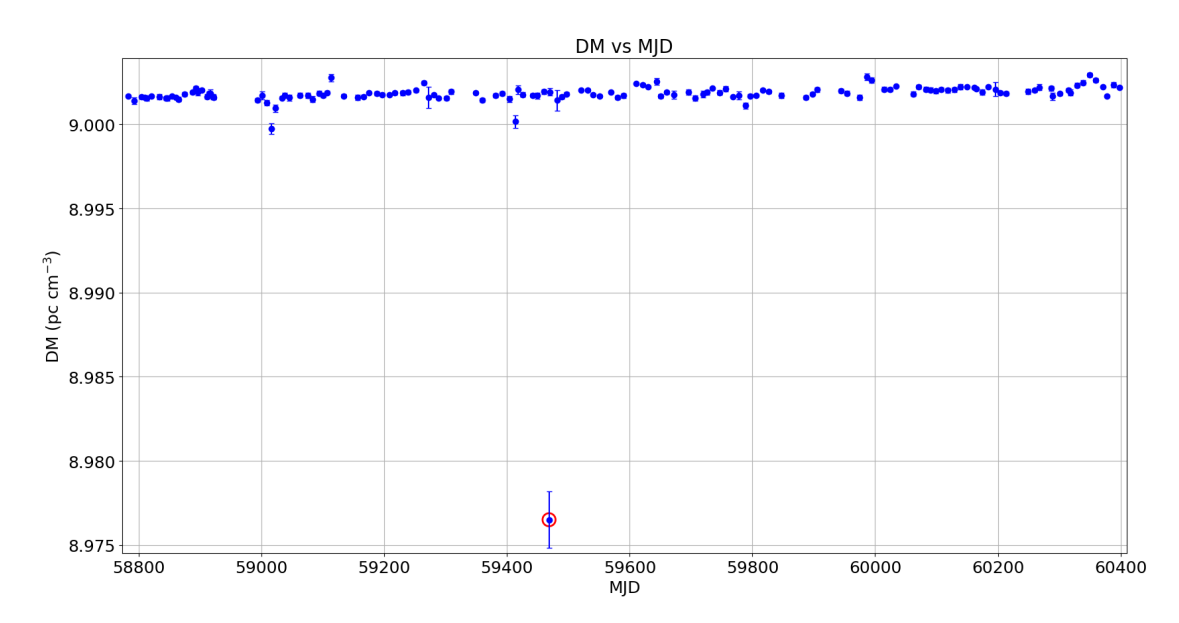


Figure 6: DM time series of PSR J2145-0750 along the InPTA-DR2 baseline (all prominent outliers, which are artifacts of poor data, are not included in this plot), highlighting the single outlier, corresponding to a potential mode-change, with red circle.

4.1 Peak-ratio distribution

For each observational epoch, we updated the corresponding archive/fits files using the InPTA-DR2 final timing solution. The header DM values were then corrected with epoch-wise estimates obtained from DMCalc, and the profiles were subsequently dedispersed to remove dispersion-induced artifacts. For ready comparison and consistent analysis of all the profiles across the baseline, we positioned them at the same pulse-phase (kept the main peaks at the center). In addition, the profiles were band-equalized [40] so that the power remained uniform across the frequency channels.

We then quantified the mode of the pulse profile by evaluating the peak ratio, defined as the ratio of the left peak to the right peak in the two prominent components of the profile, for each epoch. The resulting distribution of the ratio of the component amplitudes is well described by a Gaussian with mean and mode value of 1.0698 and a standard deviation of 0.0486, yielding 1- σ bounds of [1.0212, 1.1183] (see Fig. 7). However, we identify a singular 'outlier', lying outside the Gaussian envelope, with a peak ratio of \sim 0.8, observed at MJD 59468 (11 September 2021), the same outlier seen in the DM time series plot in Fig. 6, indicative of a possible mode change. A direct comparison of the profiles across the following selected epochs confirms this interpretation (see Fig. 8). In particular, the profile at MJD 59468 shows distinctively different relative peak heights compared to those for MJD 58820 (close to the mode value of the peak-ratio distribution) and MJD 59706 or MJD 59264 (close to the 1- σ bounds). These four epochs are analyzed in detail for comparative study in the subsequent discussion.

4.2 Profile evolution with frequency

To further test the robustness of the above result, we frequency collapsed the profiles of the four epochs into eight subbands and evaluated the peak ratio in each subband. We find that, across all epochs, the profile evolution with frequency is preserved: the left peak is smaller

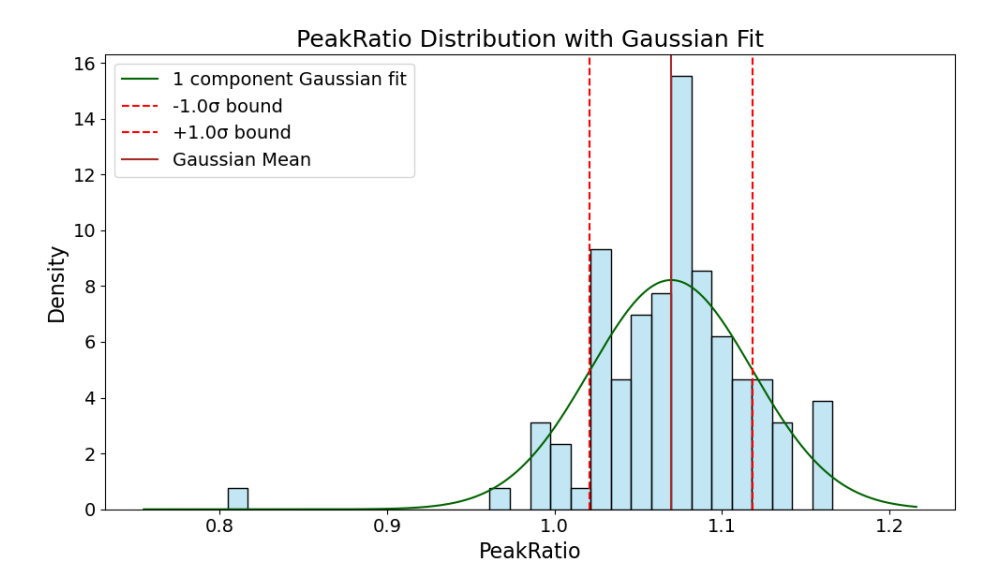


Figure 7: PSR J2145-0750 peak ratio distribution. The dark green curve is the Gaussian fit to the histogram of peak-ratio, with the two red vertical lines indicating 1- σ away from the mean peak-ratio, indicated by brown vertical line.

than the right peak at low frequencies, while the relative amplitudes gradually invert towards the higher subbands. Although the overall frequency dependence is similar, the relative peak heights at epoch MJD 59468 remain distinct from those of the other epochs, as illustrated in Fig. 9. For all the four epochs in this analysis, the number of phase bins (nbin) have been collapsed to 128 from their initially higher number of phase bins – this ensures reduction in the noise floor, and eliminates the possibility of such a mode change being an artifact of the radiometer noise.

4.3 Eliminating systematics degenerate with mode change

The peak-ratio distribution reveals a single stable mode, well described by a Gaussian, and a distinct outlier corresponding to the epoch MJD 59468. The latter lies outside the Gaussian envelope and therefore raises the natural question of whether this deviation represents a genuine mode-change event or merely an artifact arising from observational systematics. Potential sources of such artifacts include: inter-stellar dispersion, which can alter the pulse shape; inter-stellar scintillation, which modulates the pulsar signal across frequency channels and can affect the frequency-integrated profile (particularly relevant for J2145–0750, which exhibits strong frequency-dependent profile variations); polarization calibration errors or flips in polarization channels; and radiometer noise, which may distort the band shape or modify the root-mean-square (RMS) of the profile baseline.

Each of these systematics has been carefully accounted for as follows. Dispersion effects are eliminated by using highly precise, epoch-wise DM estimates obtained with DMCalc on dual-band observations. Scintillation is accounted for by inspecting subbanded profiles for the four epochs of interest, which averages out the variation in signal strength across frequency channels. Band-shape equalization and phase bin collapsing suppress the impact of radiometer noise by reducing the RMS of the noise floor. The polarization calibration related systematics would be ineffective in our dataset since they are total intensity data rather

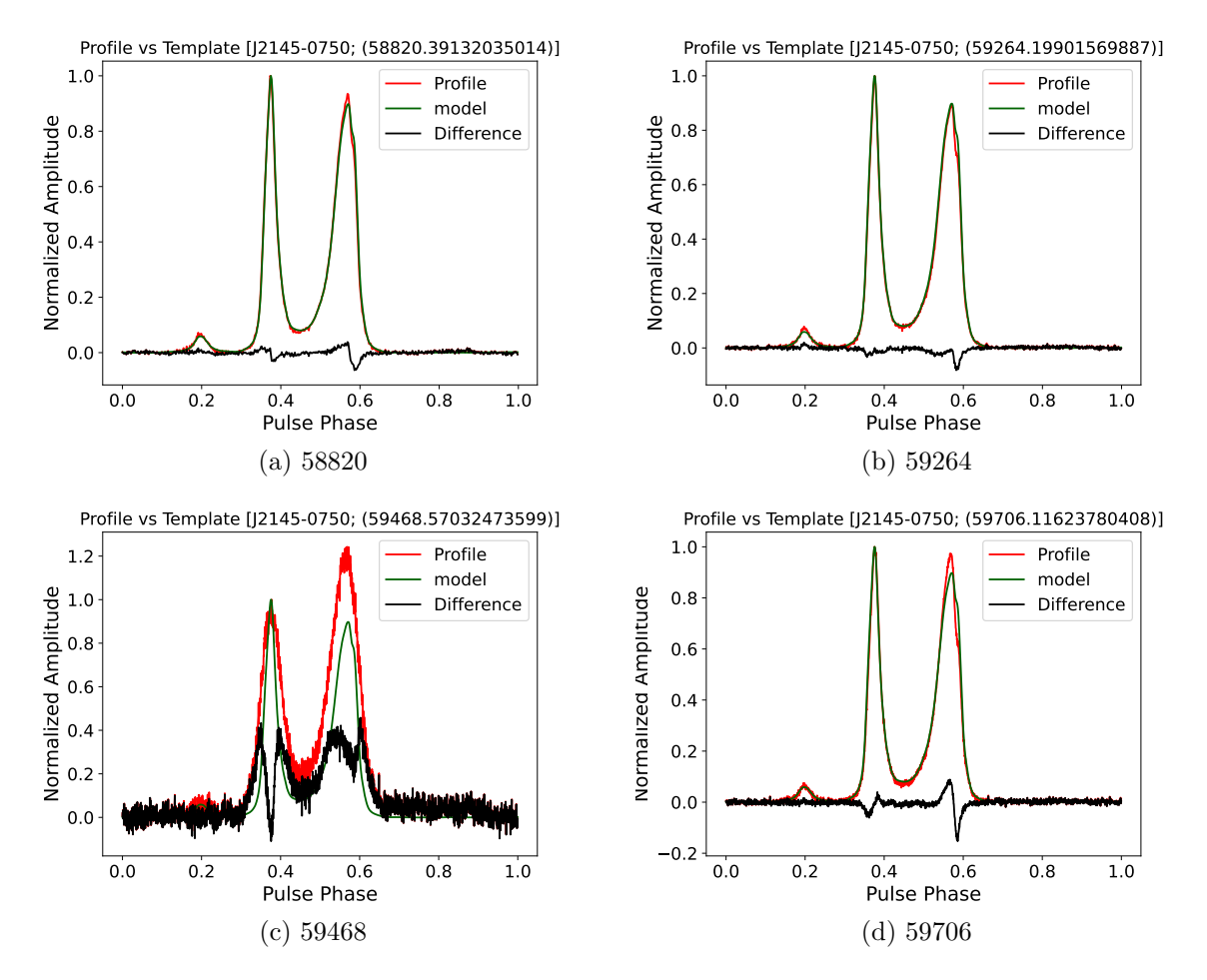


Figure 8: Profile comparison: The green curve in each of the above plots is the InPTA-DR2 template profile, while the red ones are the profiles corresponding to the epochs of interest, with the black curve denoting the difference between the profile and the template The left prominent peak component of each profile is normalized to unity for ready comparison.

than the full four Stokes parameter recordings. It is for this reason, however, an intrinsic profile change in polarized components would remain undetected in our data. Additionally, PSR J2145-0750 was at a separation angle of $\sim 160^\circ$ with the Sun, at the potential mode-changing epoch MJD 59468, thereby ruling out any solar origin for this outlier. Furthermore, we checked the observatory settings and the observatory logs for that epoch MJD 59468 – we found no mention of any observatory related glitches or atmospheric events, that could have attributed to such a potential mode change; also the observatory settings for that day was the standard one used for InPTA observations.

4.4 Indication of potential intrinsic magnetospheric changes

Apart from the change in the relative heights of the peaks of the profile we also see a *symmetric* broadening of the pulse width. We explore this, as a final test, to establish the plausible theoretical reason behind the potential mode change. We convolve each of the subbands of the template with a symmetric Gaussian kernel and find the best fit (using χ^2 test) which resembles the actual subbanded profile. The standard deviation (σ) of the best-fit Gaussian

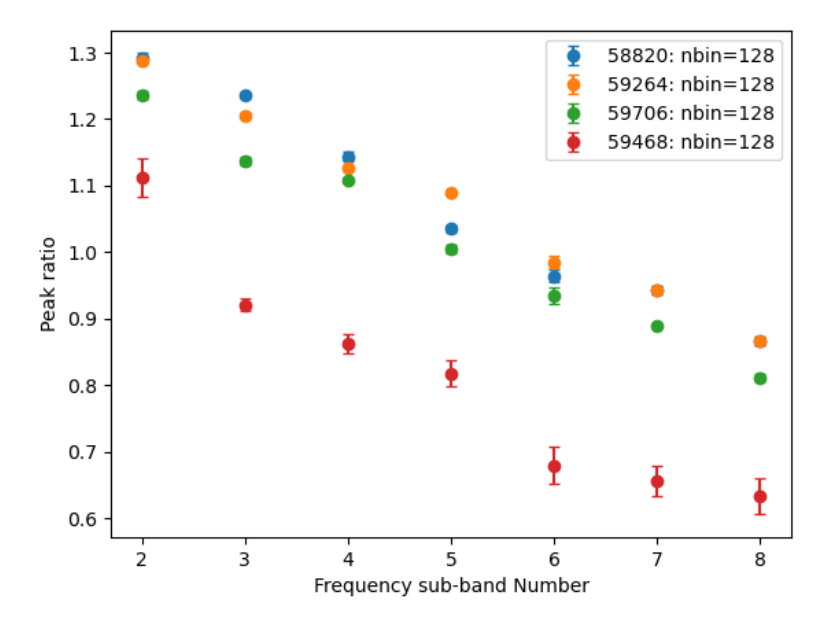


Figure 9: Profile evolution with frequency corresponding to the four epochs - MJD 58820, 59264, 59706, 59468. The X-axis corresponds to the seven out of eight subbands spanning 200 MHz band width, running from 500 MHz to 300 MHz – subband number 1 (which is removed because of noise) corresponds to a central frequency of \sim 486 MHz, and the subband number 8 corresponds to \sim 311 MHz.

kernel⁵ provides an estimate of the *observed* broadening in the corresponding subbanded profile. From the results of this analysis (see Fig. 10), we find non-zero σ (in bin units) for each of the subbands.

When we fit the subbanded σ s with a power law, we find its frequency dependence as $\sigma \propto \nu^{-2.91}$, which is different from that due to any known propagation effect. In fact, for a non-outlying epoch, say MJD 58820 (mode of the peak-ratio distribution), the absence of any such visible pulse-width broadening, comes in support for the potential mode changing event. From the σ value of each subband we could deduce an estimate of the possible deviation in the DM value (ΔDM). For that we equate the residual dispersion delay ($\Delta t_{\Delta DM}$) across a subband, owing to DM variability, with the observed profile-broadening, σ , for that particular subband:

$$\Delta t_{\Delta DM} \ (ms) = 8.3 \times 10^6 \times \Delta DM \times \frac{\Delta \nu}{\nu^3} = \sigma \ (ms) = \sigma \ (bins) \times \frac{P}{nbin} \ ,$$
 (4.1)

where P is the pulsar spin period, $\Delta\nu$ is the width of the subband, with ν being the central frequency of the subband. We observe that the estimated $\Delta DM \sim 0.08~pc/cc$, for all the subbands, exceeds the uncertainty $\sim 0.001~pc/cc$ in DM evaluation using DMCalc, by nearly two orders of magnitude. Hence, such a huge error⁶ in DM would have been clearly visible as

⁵The parameters for the Gaussian convolution is $\{A, B, s, \sigma\}$, where A is the amplitude, B is the base line offset, s is the phase-shift.

 $^{^6}$ here by DM-error we refer to the difference in true DM and DMCalc-evaluated DM, while by DM-uncertainty we refer to the confidence interval on our DMCalc-evaluated DM value.

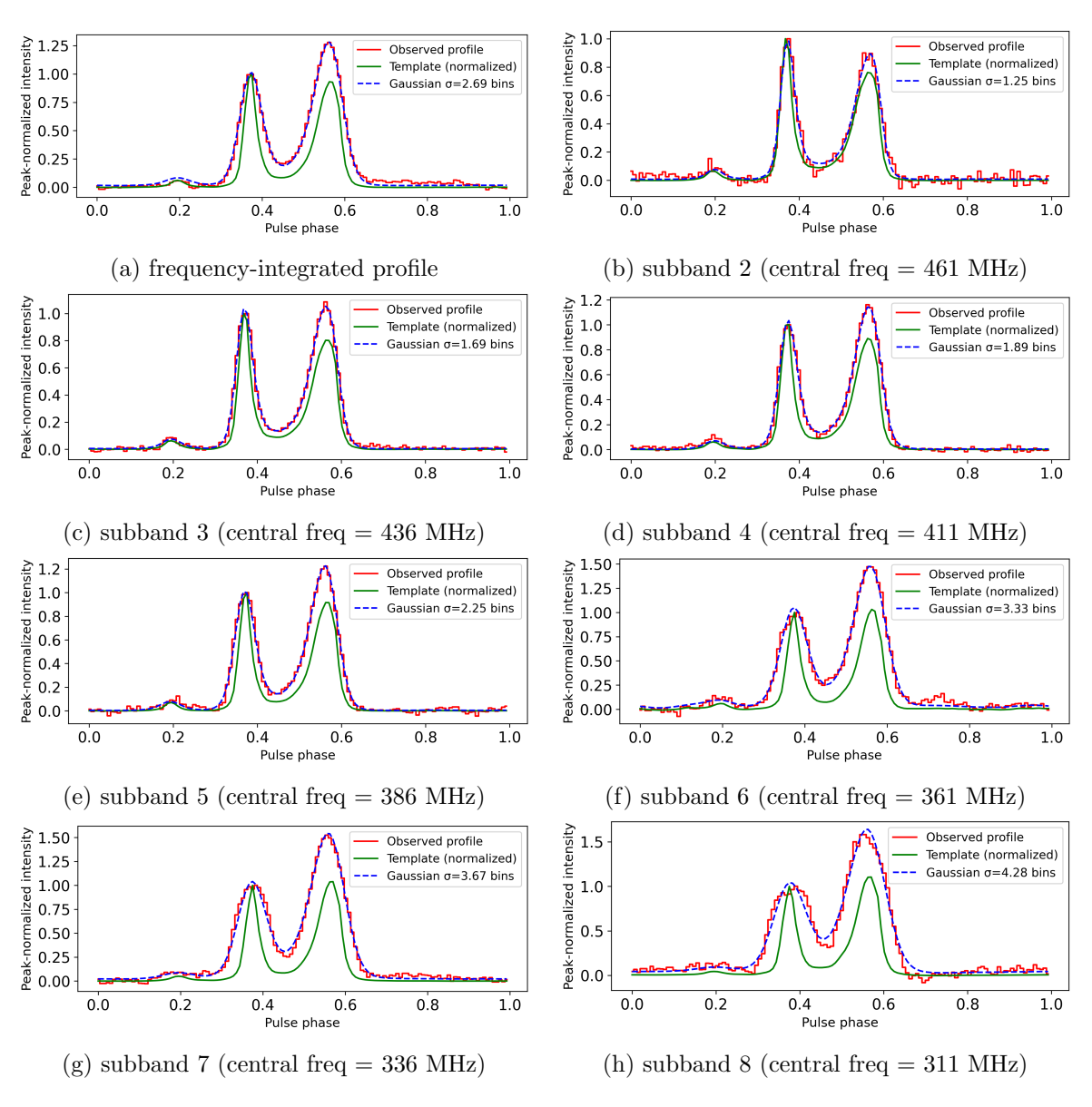


Figure 10: Convolution plots: The green curve in each of the above plots is the InPTA-DR2 template profile for the full band in (a) and corresponding subbands from (b)-(h), while the red ones are the profiles corresponding to the full band in (a) and subbands in (b)-(h). The blue dashed curve is the best-fit convolved template with a Gaussian kernel. Subband 1 is not considered since it has poor S/N.

a parabolic drift in the frequency-phase plot of the dedispersed frequency-integrated profile, which we do not see. Therefore, the source for the observed pulse-width broadening is less likely to be due to dispersion effects. Scattering effect, if any, is also possibly not the dominating contributor to such a pulse-width broadening, as validated from the absence of well-defined asymmetric exponential tails of the individual pulses in the profile and that clear scintles of 3–4 MHz wide scintillation bandwidths were seen in the observations. The symmetric broadening in the pulse-widths, therefore, in all possibilities, indicate a potential magnetospheric origin [56, 57].

5 Conclusions

In this work, we investigated astrophysically motivated outliers in the InPTA-DR2 DM time series, focusing on two representative pulsars: PSR J1022+1001 and PSR J2145-0750. We demonstrated that such outliers can serve as powerful probes of diverse plasma processes along the line of sight as well as intrinsic changes in a pulsar.

For PSR J1022+1001, we identified a distinct DM excursion on MJD 59800 (09 August 2022), which is geometrically consistent with a coronal mass ejection (CME) event detected by LASCO/C3 coronagraph, STEREO-A satellite and the DONKI database. Quantitative comparison between the DM excess inferred from radio data and that derived from in situ solar plasma measurements revealed excellent agreement, strongly establishing one of the first direct radio signatures of a CME along this particular PTA pulsar's line of sight. This result underscores the potential for tracing heliospheric plasma dynamics and properties from the PTA datasets at astronomical distances where satellites are not present. Additionally, the number of IPTA pulsars monitored all across the sky is large enough, compared to spacebased satellites, to possibly generate a three dimensional understanding of the outflow and interactions of solar wind and CMEs. The combination of several PTA datasets, across larger baselines, has the potential to contain more such solar-activity-induced outliers - this present understanding will therefore help in better modelling of the red-noise in the PTA dataset, induced by solar activities. This will lead to more accurate timing without having to throw away a significant portion of the dataset, at low separation angles, in the absence of better solar wind modelling.

For PSR J2145-0750, the analysis of high S/N profiles revealed a statistically significant outlier in the peak-ratio distribution at MJD 59468 (11 September 2021), corresponding to a clear change in the relative amplitudes and widths of the two principal pulse components. Systematic checks indicated that the broadening and altered peak ratio are possibly intrinsic to the pulsar. The observed frequency dependence of the symmetric pulse-width broadening, further supports a possible magnetospheric origin rather than propagation effects. Since our analysis is restricted to total intensity data, we cannot directly assess whether the observed mode change is associated with changes in the polarization components. The event likely represents a short-lived mode-change, which left its imprint on the band 3 prominently, marking the first such indication for this source within the InPTA frequency band. This study underscores the importance of recognizing such mode-changing behavior in, not only PSR J2145-0750, but also, other pulsars in the PTA datasets, and analyzing them further for deeper understanding of such transients. Studying the physical origins of such modechanges paves the path towards better timing and thus noise modelling, without having to discard potential outliers in efforts to make the data ready for Gravitational wave background (GWB) analysis.

Together, these results highlight the dual scientific potential of PTA observations: as sensitive detectors of solar plasma phenomena and as monitors of intrinsic pulsar magnetospheric variability. The methodology developed here – combining detection of scientific DM-outliers, analyzing solar event data, and frequency-resolved profile analysis – can be systematically extended to the full InPTA-DR2 sample to uncover additional transient phenomena.

Future work will focus on (i) expanding this framework to other InPTA-DR2 pulsars with low ecliptic latitudes to identify further CME-related DM excursions, (ii) incorporating polarization and higher time-resolution data to explore the rotation variations due to solar events as well as physical triggers of mode changes, (iii) correlating DM and profile variability, and (iv) incorporating these propagation and intrinsic effects into the timing and noise modelling for PTA science. These efforts will deepen our understanding of both the heliospheric plasma environment and the dynamic magnetospheres of millisecond pulsars, thereby improving PTA data fidelity for gravitational-wave detection.

Acknowledgments

The authors acknowledge the use of data from the STEREO mission, obtained through the CDAWeb service of NASA's Space Physics Data Facility (SPDF). We thank Christina Lee (UCB/SSL), Dr. Antoinette Galvin (University of New Hampshire), and the CDAWeb team for providing access to the in situ data used in this paper. SC and MB thank the Department of Atomic Energy for its support in hosting "Decoding Outliers and Taming Jitters: A Deep Dive into InPTA Data" through Apex-I Project - Advance Research and Education in Mathematical Sciences at IMSc. During this workshop, a significant fraction of the work presented in this paper was carried out. AKP is supported by CSIR fellowship Grant number 09/0079(15784)/2022-EMR-I. AmS is supported by CSIR fellowship Grant number 09/1001(12656)/2021-EMR-I. AS and KR are supported by UGC JRF fellowship. BCJ acknowledges the support from Raja Ramanna Chair fellowship of the Department of Atomic Energy, Government of India (RRC – Track I Grant 3/3401 Atomic Energy Research 00 004 Research and Development 27 02 31 1002//2/2023/RRC/R&D-II/13886 and 1002/2/2023/RRC/R&D-II/14369). BCJ also acknowledges support from the Department of Atomic Energy Government of India, under project number 12-R&D-TFR-5.02-0700. HT is supported by DST INSPIRE Fellowship, INSPIRE code IF210656. KV is supported by CSIR JRF Fellowship. KT is partially supported by JSPS KAKENHI Grant Numbers 20H00180, 21H01130, 21H04467, and 24H01813, and Bilateral Joint Research Projects of JSPS (120237710). NDB is supported by DST-WISE fellowship (DST/WISE-PDF/PM-17/2024). SD is supported by SERB MTR/2023/000384. ZZ is supported by the Prime Minister's Research Fellows (PMRF) scheme, Ref. No. TF/PMRF-22-7307.

References

- [1] J. P. W. Verbiest, S. J. Vigeland, N. K. Porayko, S. Chen and D. J. Reardon, Status report on global pulsar-timing-array efforts to detect gravitational waves, Results in Physics 61 (2024) 107719 [2404.19529].
- [2] W. A. Coles et al., Pulsar Observations of Extreme Scattering Events, Astrophys. J. 808 (2015) 113 [1506.07948].

- [3] N. D. R. Bhat, S. M. Ord, S. E. Tremblay, S. J. McSweeney and S. J. Tingay, Scintillation arcs in low-frequency observations of the timing-array millisecond pulsar psr j0437-4715, The Astrophysical Journal 818 (2016) 86.
- [4] Y. Liu, J. P. W. Verbiest, R. A. Main, Z. Wu, K. M. Ambalappat, D. J. Champion et al., Long-term scintillation studies of EPTA pulsars. I. Observations and basic results, A & A 664 (2022) A116 [2203.16950].
- [5] T. A. Howard, K. Stovall, J. Dowell, G. B. Taylor and S. M. White, Measuring the Magnetic Field of Coronal Mass Ejections Near the Sun Using Pulsars, Ap.J. 831 (2016) 208.
- [6] C. Tiburzi, G. M. Shaifullah, C. G. Bassa, P. Zucca, J. P. W. Verbiest, N. K. Porayko et al., The impact of solar wind variability on pulsar timing, A & A 647 (2021) A84 [2012.11726].
- [7] I. C. Niţu, M. J. Keith, C. Tiburzi, M. Brüggen, D. J. Champion, S. Chen et al., A Gaussian-processes approach to fitting for time-variable spherical solar wind in pulsar timing data, MNRAS 528 (2024) 3304 [2401.07917].
- [8] C. Tiburzi and J. P. W. Verbiest, The effect of the Solar wind on low-frequency observations of pulsars, in Pulsar Astrophysics the Next Fifty Years, P. Weltevrede, B. B. P. Perera, L. L. Preston and S. Sanidas, eds., vol. 337 of IAU Symposium, pp. 279–282, Aug., 2018, 1804.04040, DOI.
- [9] H. Grover, B. C. Joshi, J. Singha, E. Gügercinoğlu, P. Arumugam, D. Bandyopadhyay et al., The ORT and the uGMRT pulsar monitoring program: Pulsar timing irregularities & the Gaussian process realisation, PASA 41 (2024) e102 [2405.14351].
- [10] H. Grover, E. Gügercinoğlu, B. C. Joshi, M. A. Krishnakumar, S. Desai, P. Arumugam et al., Post-glitch Recovery and the Neutron Star Structure: The Vela Pulsar, arXiv e-prints (2025) arXiv:2506.02100 [2506.02100].
- [11] R. F. Mandow, A. Zic, J. R. Dawson, S. Wang, M. Curylo, S. Dai et al., *Ultra-Wideband Polarimetry of the April 2021 Profile Change Event in PSR J1713+0747*, arXiv e-prints (2025) arXiv:2509.18972 [2509.18972].
- [12] M. T. Miles, R. M. Shannon, M. Bailes, D. J. Reardon, S. Buchner, H. Middleton et al., Mode changing in J1909 - 3744: the most precisely timed pulsar, MNRAS 510 (2022) 5908 [2112.00897].
- [13] M. T. Lam, Evidence for multiple pulse-shape changes during the third chromatic timing event of psr j1713 + 0747, Research Notes of the AAS 5 (2021) 167.
- [14] B. Goncharov, D. J. Reardon, R. M. Shannon, X.-J. Zhu, E. Thrane, M. Bailes et al., Identifying and mitigating noise sources in precision pulsar timing data sets, MNRAS 502 (2021) 478 [2010.06109].
- [15] J. Singha, M. P. Surnis, B. C. Joshi, P. Tarafdar, P. Rana, A. Susobhanan et al., Evidence for profile changes in PSR J1713+0747 using the uGMRT, MNRAS 507 (2021) L57 [2107.04607].
- [16] R. J. Jennings, J. M. Cordes, S. Chatterjee, M. A. McLaughlin, P. B. Demorest,
 Z. Arzoumanian et al., An Unusual Pulse Shape Change Event in PSR J1713+0747 Observed with the Green Bank Telescope and CHIME, ApJ 964 (2024) 179 [2210.12266].
- [17] M. A. Krishnakumar, P. K. Manoharan, B. C. Joshi, R. Girgaonkar, S. Desai, M. Bagchi et al., High precision measurements of interstellar dispersion measure with the upgraded GMRT, Astronomy & Astrophysics 651 (2021) A5.
- [18] A. Srivastava, S. Desai, N. Kolhe, M. Surnis, B. C. Joshi, A. Susobhanan et al., Noise analysis of the Indian Pulsar Timing Array data release I, Physical Review D. 108 (2023) 023008 [2303.12105].

- [19] B. C. Joshi, P. Arumugasamy, M. Bagchi, D. Bandyopadhyay, A. Basu, N. D. Batra et al., Precision pulsar timing with the ORT and the GMRT and its applications in pulsar astrophysics, Journal of Astrophysics and Astronomy 39 (2018) 51.
- [20] B. C. Joshi, A. Gopakumar, A. Pandian, T. Prabu, L. Dey, M. Bagchi et al., *Nanohertz* gravitational wave astronomy during SKA era: An InPTA perspective, Journal of Astrophysics and Astronomy 43 (2022) 98 [2207.06461].
- [21] D. J. Champion, G. B. Hobbs, R. N. Manchester, R. T. Edwards, D. C. Backer, M. Bailes et al., *Measuring the Mass of Solar System Planets Using Pulsar Timing*, *ApJL* **720** (2010) L201 [1008.3607].
- [22] R. N. Caballero, Y. J. Guo, K. J. Lee, P. Lazarus, D. J. Champion, G. Desvignes et al., Studying the Solar system with the International Pulsar Timing Array, MNRAS 481 (2018) 5501 [1809.10744].
- [23] L. Li, L. Guo and G.-L. Wang, Detecting the errors in solar system ephemeris by pulsar timing, Research in Astronomy and Astrophysics 16 (2016) 58.
- [24] Y. J. Guo, G. Y. Li, K. J. Lee and R. N. Caballero, Studying the Solar system dynamics using pulsar timing arrays and the LINIMOSS dynamical model, MNRAS 489 (2019) 5573 [1909.04507].
- [25] K. J. Lee, Pulsar timing arrays and gravity tests in the radiative regime, Classical and Quantum Gravity 30 (2013) 224016.
- [26] N. J. Cornish, L. O'Beirne, S. R. Taylor and N. Yunes, Constraining Alternative Theories of Gravity Using Pulsar Timing Arrays, Phys. Rev. Lett. 120 (2018) 181101 [1712.07132].
- [27] Q. Liang, M.-X. Lin and M. Trodden, A test of gravity with Pulsar Timing Arrays, JCAP **2023** (2023) 042 [2304.02640].
- [28] Q. Liang, I. Obata and M. Sasaki, Testing gravity with frequency-dependent overlap reduction function in Pulsar Timing Array, JCAP 2024 (2024) 097 [2405.11755].
- [29] P. B. Demorest, T. Pennucci, S. M. Ransom, M. S. E. Roberts and J. W. T. Hessels, A two-solar-mass neutron star measured using Shapiro delay, Nature 467 (2010) 1081 [1010.5788].
- [30] M. Kramer and D. J. Champion, The European Pulsar Timing Array and the Large European Array for Pulsars, Classical and Quantum Gravity 30 (2013) 224009.
- [31] R. N. Manchester, G. Hobbs, M. Bailes, W. A. Coles, W. van Straten, M. J. Keith et al., *The Parkes Pulsar Timing Array Project*, *PASA* **30** (2013) e017 [1210.6130].
- [32] M. A. McLaughlin, The North American Nanohertz Observatory for Gravitational Waves, Classical and Quantum Gravity 30 (2013) 224008 [1310.0758].
- [33] M. T. Miles, R. M. Shannon, D. J. Reardon, M. Bailes, D. J. Champion, M. Geyer et al., The MeerKAT Pulsar Timing Array: the first search for gravitational waves with the MeerKAT radio telescope, MNRAS 536 (2025) 1489 [2412.01153].
- [34] S. Chen, H. Xu, Y. Guo, B. Wang, R. N. Caballero, J. Jiang et al., *The Chinese Pulsar Timing Array Data Release I: Single pulsar noise analysis*, A & A 699 (2025) A165 [2506.04850].
- [35] G. Hobbs, A. Archibald, Z. Arzoumanian, D. Backer, M. Bailes, N. D. R. Bhat et al., The International Pulsar Timing Array project: using pulsars as a gravitational wave detector, Classical and Quantum Gravity 27 (2010) 084013 [0911.5206].
- [36] G. Agazie, A. Anumarlapudi, A. M. Archibald, Z. Arzoumanian, P. T. Baker, B. Bécsy et al., The NANOGrav 15 yr Data Set: Evidence for a Gravitational-wave Background, ApJL 951 (2023) L8 [2306.16213].

- [37] EPTA Collaboration, InPTA Collaboration, J. Antoniadis, P. Arumugam, S. Arumugam, S. Babak et al., The second data release from the European Pulsar Timing Array. III. Search for gravitational wave signals, A & A 678 (2023) A50 [2306.16214].
- [38] H. Xu, S. Chen, Y. Guo, J. Jiang, B. Wang, J. Xu et al., Searching for the Nano-Hertz Stochastic Gravitational Wave Background with the Chinese Pulsar Timing Array Data Release I, Research in Astronomy and Astrophysics 23 (2023) 075024 [2306.16216].
- [39] D. J. Reardon, A. Zic, R. M. Shannon, G. B. Hobbs, M. Bailes, V. Di Marco et al., Search for an Isotropic Gravitational-wave Background with the Parkes Pulsar Timing Array, ApJL 951 (2023) L6 [2306.16215].
- [40] P. Rana, P. Tarafdar, K. Nobleson, C. Dwivedi, B. Chandra Joshi, D. Deb et al., The Indian Pulsar Timing Array data release 2: I. Dataset and timing analysis, PASA 42 (2025) e108 [2506.16769].
- [41] P. Tarafdar, K. Nobleson, P. Rana, J. Singha, M. A. Krishnakumar, B. C. Joshi et al., *The Indian Pulsar Timing Array: First data release*, *PASA* **39** (2022) e053 [2206.09289].
- [42] Y. Gupta, B. Ajithkumar, H. S. Kale, S. Nayak, S. Sabhapathy, S. Sureshkumar et al., *The upgraded GMRT: Opening new windows on the radio Universe, Current Science* **113** (2017) 707.
- [43] K. De and Y. Gupta, A real-time coherent dedispersion pipeline for the giant metrewave radio telescope, Experimental Astronomy 41 (2016) 67 [1509.00186].
- [44] A. Susobhanan, Y. Maan, B. C. Joshi, T. Prabu, S. Desai, K. Nobleson et al., pinta: The uGMRT data processing pipeline for the Indian Pulsar Timing Array, PASA 38 (2021) e017 [2007.02930].
- [45] C. L. Kuo and L. C. Lee, Ionospheric plasma dynamics and instability caused by upward currents above thunderstorms, Journal of Geophysical Research (Space Physics) 120 (2015) 3240.
- [46] P. Richard, A. Delannoy, G. Labaune and P. Laroche, Results of spatial and temporal characterization of the VHF-UHF radiation of lightning, Journal of Geophysical Research 91 (1986) 1248.
- [47] M. Hesse, M. Kuznetsova, L. Rastaetter and P. MacNeice, Space Weather Models at the CCMC And Their Capabilities, in AGU Fall Meeting Abstracts, vol. 2007 of AGU Fall Meeting Abstracts, pp. SM43E-03, Dec., 2007.
- [48] M. L. Kaiser, T. A. Kucera, J. M. Davila, O. C. St. Cyr, M. Guhathakurta and E. Christian, The STEREO Mission: An Introduction, Space Science Rev 136 (2008) 5.
- [49] D. Odstrcil, Modeling 3-D solar wind structure, Advances in Space Research 32 (2003) 497.
- [50] C. N. Arge and V. J. Pizzo, Improvement in the prediction of solar wind conditions using near-real time solar magnetic field updates, Journal of Geophysical Research 105 (2000) 10465.
- [51] D. Odstrcil, P. Riley and X. P. Zhao, Numerical simulation of the 12 May 1997 interplanetary CME event, Journal of Geophysical Research (Space Physics) 109 (2004) A02116.
- [52] G. E. Brueckner, R. A. Howard, M. J. Koomen, C. M. Korendyke, D. J. Michels, J. D. Moses et al., *The Large Angle Spectroscopic Coronagraph (LASCO)*, *Solar Physics* **162** (1995) 357.
- [53] S. A. Maloney and P. T. Gallagher, Solar Wind Drag and the Kinematics of Interplanetary Coronal Mass Ejections, ApJL 724 (2010) L127 [1010.0192].
- [54] P. Subramanian, A. Lara and A. Borgazzi, Can solar wind viscous drag account for coronal mass ejection deceleration?, Geophysical Research Letters 39 (2012) L19107 [1209.2595].
- [55] C.-H. Lin and J. Chen, Drag Force on Coronal Mass Ejections (CMEs), Journal of Geophysical Research (Space Physics) 127 (2022) e28744.

- [56] A. Lyne, G. Hobbs, M. Kramer, I. Stairs and B. Stappers, Switched Magnetospheric Regulation of Pulsar Spin-Down, Science 329 (2010) 408 [1006.5184].
- [57] A. N. Timokhin, A model for nulling and mode changing in pulsars, MNRAS 408 (2010) L41 [0912.2995].